LL-37-induced host cell cytotoxicity depends on cellular expression of the globular C1q receptor (p33).

Svensson, Daniel; Wilk, Laura; Mörgelin, Matthias; Herwald, Heiko; Nilsson, Bengt-Olof

Published in:
The Biochemical journal

DOI:
10.1042/BJ20150798

2016

LL-37-induced host cell cytotoxicity depends on cellular expression of the globular C1q receptor (p33)

Daniel Svensson*, Laura Wilk†, Matthias Mörgelin†, Heiko Herwald†, and Bengt-Olof Nilsson*

*Department of Experimental Medical Science, Lund University, BMC D12, SE-22184 Lund, Sweden
†Department of Clinical Sciences, Division of Infection Medicine, Lund University, BMC C14, SE-22184 Lund, Sweden

Short title: p33 protects host cells against LL-37-induced cytotoxicity

To whom correspondence should be addressed: Dr. Bengt-Olof Nilsson
Department of Experimental Medical Science
Lund University
BMC D12
SE-221 84 Lund
Sweden
Phone: +46-46-2227767
Fax: +46-46-2224546
E-Mail: bengt-olof.nilsson@med.lu.se

ABSTRACT

The human host-defense peptide LL-37 not only displays antimicrobial activity but also immune modulating properties that trigger intracellular signaling events in host cells. Since the cytolytic activity of high LL-37 concentrations affects cell viability, the function of LL-37 requires tight regulation. Eukaryotic cells therefore benefit from protective measures to prevent harmful effects of LL-37. p33, also known as globular C1q receptor, is reported to act as an LL-37 antagonist by binding the peptide thereby reducing its cytotoxic activity. In this report, we show that high levels of endogenous p33 correlate with an increased viability in human cells treated with LL-37. Sub-cellular localization analysis showed p33 distribution at the mitochondria, the plasma membrane and in the cytosol. Strikingly, cytosolic over-expression of p33 significantly antagonized detrimental effects of LL-37 on cell fitness, while the reverse effect was observed by siRNA-induced down-regulation of p33. However, modulation of p33 expression had no effect on LL-37-induced plasma membrane pore forming capacity pointing to an intracellular mechanism. A scavenging function of intracellular p33 is further supported by co-immunoprecipitation experiments, showing a direct interaction between intracellular p33 and LL-37. Thus, our findings support an important role of intracellular p33 in maintaining cell viability by counteracting LL-37-induced cytotoxicity.

Keywords: antimicrobial peptide (AMP), gC1qR, host defense, innate immunity, keratinocyte, osteoblast

Summary statement: It is unclear how human host cells cope with cytotoxic effects caused by the host-defense peptide LL-37. Our findings show that LL-37-induced cytotoxicity is counteracted by intracellular p33, suggesting that p33 protects against deleterious activities of the innate immune system.

INTRODUCTION

Host-defense peptides (HDPs) are at the forefront of innate immune defense mechanisms against microbial infections. Although initially believed to be solely involved in disrupting bacterial cell membranes, it is now clear that their functions in the host response to infection are far more complex (for a review see [1]). For instance, HDPs have been revealed to trigger inflammatory reactions in eukaryotic cells [2], act as chemoattractant [3], or promote cellular differentiation [4].

The cathelicidins represent one family of HDPs, with hCAP-18 as the only currently known human member [1]. As for all cathelicidins, hCAP-18 represents a two domain pro-peptide-form, from which the C-terminal peptide is released [1]. hCAP-18 is produced by epithelial cells and neutrophils and upon exocytosis processed to the HDP LL-37 by proteinase 3, which is secreted from activated neutrophils [2, 3]. LL-37 possesses both hydrophobic and hydrophilic properties [5], and exerts its antimicrobial effects through disruption of the bacterial cell wall causing cell lysis of both Gram-negative and Gram-positive bacteria and by neutralizing bacterial lipopolysaccharides [6-8]. Apart from its antimicrobial properties, LL-37 has been reported to influence inflammatory cell recruitment, modulate TLR function and type I interferon responses, and play a role in autoimmunity (for a review see [9]).

Under pathological conditions, high levels of LL-37 have been found to reduce cell viability and promote apoptosis in osteoblasts, vascular smooth muscle cells, periodontal ligament cells, neutrophils, airway epithelial cells and T cells [10-15]. Notably, very high concentrations, exceeding several 100 μM of LL-37, have been detected in lesions from patients suffering from the autoimmune diseases psoriasis, rosacea and ulcerative colitis, suggesting an important role of LL-37 in these disease processes [16-18]. Also under other inflammatory conditions, such as chronic periodontitis, concentrations of LL-37 can locally reach levels within the micromolar range [19].

In order to counteract the detrimental effects evoked by LL-37, the host relies on endogenous mechanisms. Though this area of research is not widely explored, one putative candidate in host protection is the human protein p33, also referred to as p32 or globular C1q receptor (gC1qR). p33 is expressed in different human cell types such as neutrophils, endothelial cells, lymphocytes, platelets and osteoblasts [20-22], and was originally described as a complement C1q binding protein [23, 24]. Mature p33 is comprised of 209 amino acid residues and derived from a precursor protein carrying a mitochondrial signal sequence. p33 is implied to be trimeric, with one of its two surfaces highly negatively charged due to a high number of glutamic and aspartic acids (28 and 20 amino acids, respectively) [25, 26]. Therefore, p33 was proposed to act as a scavenger for cationic HDPs such as LL-37. Indeed, exogenously applied trimeric p33 binds LL-37 and other HDPs. HDPs show high affinity for the negatively charged beta-sheet (aa 115-135) of p33, thereby neutralizing their antimicrobial activity [27]. p33 has been proposed to prevent HDP-induced cytotoxicity in endothelial cells and erythrocytes through this scavenging mechanism [27]. Moreover, exogenous p33 (1-10 μM) antagonizes LL-37-induced apoptosis in osteoblasts in a concentration-dependent manner [22].

In the present study, we show an important role of endogenous, intracellular p33 for host cell viability. We find that LL-37 differentially attenuates the viability of various cell types depending on their intracellular p33 level and demonstrate that p33 antagonizes the

detrimental effects of LL-37. Together, our results suggest that the levels of intracellular p33 determine the extent of the cellular damage caused by LL-37.

EXPERIMENTAL

Cells and cell culture

The human osteoblast-like MG63 cell line and human HeLa cells were obtained from the American Type Tissue Culture Collection (ATCC). The human keratinocyte HaCaT cell line and neonatal dermal fibroblasts (HDFa) were purchased from CLS Cell Lines Service GmbH and Cascade Biologics, respectively. The human periodontal ligament fibroblasts (PDL cells) were obtained from teeth extracted for orthodontic reasons as described previously [28]. The patients (boys and girls 14-15 years of age) and their parents were informed both orally and in writing and a written consent was signed. This procedure was approved by the Human Ethical Committee, Lund University, Lund, Sweden. The cells were cultured in DMEM/Ham´s F12 (1:1) (Life Technologies) supplemented with antibiotics (penicillin 50 U/ml, streptomycin 50 µg/ml, Biochrom GmbH) and 10% fetal bovine serum (FBS, Biochrom GmbH) and kept at 37 °C under 5% CO_2 in air in a water-jacketed cell incubator. The cells were trypsinized (0.25% Trypsin/EDTA) and counted using the Luna™ Automated Cell Counter system (Logos Biosystem) in accordance to the manufacturer's instructions. Cell morphology was evaluated in photographs obtained by a Nikon TMS phase-contrast microscope equipped with a digital camera (Pixelink, Nikon). The cell lines were used up to passage 30. The primary PDL cells were used in passages 2-4. Cells were treated with LL-37 (Bachem AG) dissolved in DMSO. Controls received DMSO-vehicle as appropriate. Identical responses to LL-37 were obtained irrespective of passage number.

Transfection with p33 siRNA

The p33 siRNA (Hs_C1QBP_6) and non-coding scramble control (All Stars Negative Control), both purchased from Qiagen, were transfected into the cells using Oligofectamine transfection reagent (Life Technologies). Briefly, an RNA/Oligofectamine mix was prepared in Opti MEM medium (Life Technologies) according to manufacturer's instructions. Cells were seeded at a density of 1.2×10^5 per culture dish and treated with p33 siRNA and scramble RNA at an RNA concentration of 20 nM for 24 and 96 h for MG63 and HaCaT cells, respectively. The cells were allowed to equilibrate under growth-stimulated conditions for 48 h followed by a second transfection as described above. The HaCaT cells were transfected for a longer time because they were less sensitive to the transfection. Cells were trypsinized and re-seeded at identical density for functional experiments in a 1:1 mixture of transfection medium and fresh culture medium.

Plasmid DNA for transient transfection

Human p33 lacking the mitochondrial signal sequence was used for transient transfections and overexpression. p33 was PCR amplified from the p33-pMAL-c2 vector described in Herwald *et al.* [20] using the following primers: The 5'-cgcggatccaccatgggcctgcacaccgacggagac-3' forward primer introduced a *Bam*HI restriction site as well as a Kozak consensus sequence, while the reverse primer 5'-ccgctcgagctactggctcttgacaaaactcttgagg-3' introduced a stop codon and a *Xho*I restriction site. PCR product and pcDNA 3.1(+) mammalian expression vector (Life Technologies) were both treated with FastDigest enzymes *Bam*HI and *Xho*I (both from Fermentas) and purified by gel

extraction (Qiagen) according to manufacturer's instructions. pcDNA 3.1-p33 expression vector was then obtained by cloning the p33 fragment into pcDNA 3.1(+) using a DNA ligation kit (Novagen). Introduction of p33 was verified by sequencing using primers based on T7 promoter and BGH Reverse primer sequences (Life Technologies).

Transient transfection of plasmid DNA

HeLa cells were seeded in 96-well or 12-well plates at a density of 1.5×10^4 or 2.0×10^5 per well, respectively, and transfected for 24 h with pcDNA3.1-p33 expression vector or pcDNA 3.1 control vector using both Lipofectamine 3000 and P3000 reagents (both from Life Technologies) according to manufacturer's instructions. Briefly, cells were transfected in Opti MEM medium using 4 µg DNA, 8 µl P3000 reagent and 6 µl Lipofectamine 3000 reagent per ml of medium (43 µl transfection mixture per well in 96 well plates and 400 µl per well in 12 well plates). Cells were left in transfection mixture for 16 h before an equal volume of DMEM supplemented with 20% FBS was added, giving 2 µg/ml as the final vector concentration. No difference in cell viability was observed between cells transfected with the pcDNA 3.1-p33 and control vector. Successful transfection and over-expression of p33 was confirmed by quantitative real-time RT-PCR and Western blotting.

MTT assay

Cell viability was assessed using the 3-(4,5-dimethylthiazol-2-yl)-2,5-diphenyl tetrazolium bromide (MTT) assay as described by Carmichael *et al*. [29]. Briefly, cells were seeded at a density of 1.5×10^4 cells/well in 96-well plates. After 24 h, cells were treated with or without LL-37 for 3 h in phenol red-free DMEM culture medium at 37 °C in a cell incubator. Phenol red was omitted since it may interfere with the absorbance reading. The LL-37-containing medium was removed and then the cells were incubated with MTT (0.5 mg/ml) in cell culture medium for 1 h at 37 °C. After 1 h, the MTT-containing medium was removed and the blue formazan product dissolved by adding 100 µl DMSO per well. Absorbance was monitored at 540 nm in a Multiscan GO Microplate Spectrophotometer (Thermo Scientific).

LDH assay

Pore formation by LL-37 was assessed by measuring the release of lactate dehydrogenase (LDH) from cells seeded in 96-well plates. Cells were incubated with or without LL-37 for 30 min in phenol red-free DMEM culture medium at 37 °C in the cell incubator. After incubation, the plate was centrifuged at 257 x *g* for 10 min and 30 µl of supernatant was transferred to a new plate. Total LDH release was obtained by cytolysis via sonication of untreated control cells. Fresh medium was utilized as a blank. A NADH solution in water (180 µl, 56 mM TRIS, 5.6 mM EGTA, and 170 µM β-NADH) was added followed by sodium pyruvate in water (20 µl, 14 mM) and the absorbance of NADH, which had not been reduced by pyruvate-LDH, was read at 340 nm in a Multiscan GO Microplate Spectrophotometer (Thermo Scientific) for 1 h at 30 °C. LDH release in response to LL-37 was normalized to total release of LDH.

Immunocytochemistry

For immunocytochemistry, cells were cultured on coverslips. After reaching 80% confluence, cells were washed with PBS, fixed in 4% (w/v) paraformaldehyde (PFA) and permeabilized in 0.2% (v/v) Triton X-100 for 10 min. Non-specific binding sites were blocked with 2%

(w/v) BSA before polyclonal antiserum to p33 raised in rabbits (custom made antibody, Innovagen AB, 1:200 dilution) was added overnight at 4 °C. The following day, cells were incubated with secondary goat anti-rabbit Alexa Fluor 555 or Alexa Fluor 488 (Invitrogen, Cat No A21428 and A11008, both 1:500 dilutions) for 2h at RT. In some experiments, cells were co-stained with the mitochondria-selective probe MitoTracker (MitoTracker Orange CM-H_2TMRos, Molecular Probes). The cells were incubated with MitoTracker (500 nM) according to manufacturer's instructions. Cells were washed with PBS, rinsed with water, and then the coverslips were mounted using Aqua-Poly/Mount mounting medium (Polysciences). The immunoreactive signal and MitoTracker staining were analyzed using both a conventional Olympus BX60 fluorescence microscope and a laser scanning confocal microscope (LSM5 PASCAL, Carl Zeiss AG). No immunoreactivity was observed after omission of the primary p33 antibody.

Immunogold electron microscopy

After washing with PBS, fixation buffer was added and cells were scraped off from the culture dish. Cells were embedded in Epon and subjected to antigen retrieval with metaperiodate [30]. Grids were blocked with 5% (v/v) goat serum diluted in 0.2% BSA (pH 7.6, Aurion) for 15 min, followed by incubation with polyclonal rabbit anti-p33 (Innovagen AB, 1:80 dilution) overnight at 4 °C. Samples were then incubated with gold-conjugated goat anti-rabbit IgG:5 nm (BBI, Cat No EM.GAR5, 1:10 dilution) for 1h at rt. This step was followed by fixation in 2% glutaraldehyde and then samples were post-stained with uranyl acetate and lead citrate. Rabbit IgG (BioLegend) was used as a negative control. Sections were examined with a transmission electron microscope (CM100 Twin, Philips) operated at a 60 kV accelerating voltage at the Core Facility for Integrated Microscopy, Panum Institute, University of Copenhagen. The images were recorded with a side-mounted Olympus Veleta camera (Olympus).

Quantitative real-time RT-PCR

Total RNA was extracted and purified using the miRNeasy kit (Qiagen). Concentration and quality of RNA was assessed using a NanoDrop 2000C spectrophotometer (Thermo Scientific). The RNA samples were subjected to one-step quantitative real-time PCR measurements using the QuantiFast SYBR Green RT-PCR kit (Qiagen) and QuantiTect primer assays (Qiagen) on a Step One Plus real-time thermal cycler (Applied Biosystems). Gene expression was calculated using the delta CT method applying glyceraldehyde-3-phosphate dehydrogenase (*GAPDH*) as the housekeeping reference gene [31]. Each sample was analyzed in duplicate. The PCR primers (QuantiTect primer assays) for p33 (Hs_C1QBP_1_SG) and GAPDH (Hs_GAPDH_2_SG) were purchased from Qiagen.

Western blotting

Cells were washed with PBS and lysed in SDS sample buffer (Tris-HCl 62.5 mM, pH 6.8, 2% (w/v) SDS, 10% (v/v) glycerol, 1 mM phenylmethylsulfonyl fluoride). The samples were sonicated for 2 × 10 s, boiled and centrifuged (16000 x *g*). Supernatants were collected and total protein content determined by the Bio-Rad DC Protein Assay to assure equal loading in each lane. The proteins were separated by SDS-PAGE using Criterion TGX Any kD precast gels (Bio-Rad) with equal amount of protein loaded in each lane. After separation, the proteins were transferred to nitrocellulose membrane by electroblotting overnight at 4 °C. The membrane was blocked in 1% casein (w/v) in TBS (Bio-Rad) and then incubated overnight

with antibodies against p33 (clone 60.11, MMS-606R; Nordic BioSite AB, Cat No 920701, 1:1000 dilution), mouse monoclonal heat shock protein 90 (Hsp90, BD Transduction Laboratories, Cat No 610418, 1:2500 dilution) and GAPDH (clone 6C5, Merck Millipore, Cat No MAB374, 1:5000 dilution). The membranes were washed three times in TBS-T, and the immunoreactive bands were visualized by chemiluminescence using a HRP-conjugated secondary anti-mouse antibody followed by SuperSignal West Femto chemiluminescence reagent (Thermo Scientific). The p33 immunospecific band was analyzed by photodensitometric scanning and normalized to Hsp90 or GAPDH serving as internal controls. Normalization of p33 immunoreactive signal to either Hsp90 or GAPDH gave identical results. Images were acquired using a LI-COR Odyssey Fc instrument (LI-COR Biosciences).

Co-immunoprecipitation

Co-immunoprecipitation of p33 and LL-37 was performed using a Pierce Classic IP Kit (Thermo Scientific) according to manufacturer's instructions. Briefly, HaCaT or HeLa cells were treated with LL-37 (10 μM) for 10 minutes before cells were washed with PBS and lysed using the wash/lysis buffer. The lysate was divided into two equal parts, one treated with anti-p33 antibody (Innovagen AB, 6 μg), and one kept as a negative control. Lysates were incubated with agitation overnight at 4 °C before antibody was retrieved with agarose beads and washed. Proteins were eluted with SDS sample buffer and LL-37 was detected by dot blots on nitrocellulose membranes, using a monoclonal antibody against LL-37 (Cathelicidin antibody OSX12, Novus Bio, Cat No NBP1-46781, 5 μg/ml), a HRP-conjugated secondary anti-mouse antibody (Cell Signaling, Cat No #7076, 1:10000 dilution) and SuperSignal West Femto chemiluminescence reagent (Thermo Scientific).

In some experiments, sub-cellular fractionation was performed previous to co-immunoprecipitation [32]. Briefly, cells were homogenized with an Ultra-Turrax homogenizer (IKA) and nuclei pelleted by centrifugation at 800 x *g* for 10 min. The supernatant was then subjected to a second centrifugation at 30 000 x *g* for 20 min in an Optima™ L-100 XP ultra-centrifuge (Beckman Coulter) to pellet the membranes. All procedures were done at 4 °C.

Statistics

Summarized data are presented as means ± SEM. Each culture well represents one biological replicate, that is, one observation (n = 1). Number of n-values is indicated in the figure legends. Statistical significance was calculated using ANOVA and Student's two-tailed t test for unpaired comparisons with Bonferroni correction for post hoc analysis as appropriate. P values <0.05 were considered significant.

RESULTS

p33 is located at the mitochondria, the plasma membrane and in the cytosol

In the first series of experiments we aimed to localize endogenous p33 in human osteoblasts and keratinocytes. To this end, osteoblast-like MG63 cells and HaCaT keratinocytes were analyzed by immunocytochemistry. As shown in Figure 1, cytoplasmic p33 immunoreactivity was detected in MG63 cells by laser scanning confocal microscopy (Figure 1A and 1B). The nuclear p33 staining was weak compared with the cytoplasmic signal, indicating cytoplasmic

rather than nuclear location of p33 (Figure 1A and 1B). HaCaT cells showed similar distribution of p33 immunoreactivity as MG63 cells (Figure 1 C). Two further human cell types investigated, human periodontal ligament fibroblasts (PDL cells), and human neonatal dermal fibroblasts (HDFa cells), also displayed a comparable expression pattern for p33 (data not shown). By employing double-staining for p33 immunoreactivity and MitoTracker for mitochondria in HaCaT cells, we found that p33 is localized to the mitochondria (Figure 1C-1E). The sub-cellular distribution of p33 was then further analyzed by immunogold labeling electron microscopy. p33 immunoreactivity in MG63 cells was found at the mitochondrial periphery, at the plasma membrane and in some parts within the cytosol (Figure 2A). A similar distribution pattern for p33 was recorded in HaCaT cells (Figure 2C). Upon treatment with p33 siRNA, only a weak p33 immunoreactive signal was observed for all sub-cellular compartments in both HaCaT and MG63 cells (Figure 2B and 2D). Furthermore, a similar sub-cellular distribution pattern for p33 as that observed in MG63 and HaCaT cells was also seen in the HDFa and PDL fibroblasts (Figure 3).

The extent of LL-37-induced cytotoxicity differs in various cell lines

Next, we tested whether the extent of cytotoxic effects caused by LL-37 varies in different human cell lines. For this purpose, MG63, HaCaT, PDL, and HDFa cells were treated with increasing concentrations of LL-37 and cell viability assessed by the MTT and LDH assay (Figure 4A-4D). The results depicted in Figure 4A and 4B reveal that a 3-hour treatment with LL-37 causes a concentration-dependent attenuation of cell viability as assessed by the MTT assay with EC_{50} values that are in the micromolar range (HaCaT = 9 μM, MG63 = 5 μM, HDFa = 4 μM, and PDL cells = 1.7 μM, respectively). These data thus show that HaCaT cells are least sensitive to LL-37-treatment, while viability of PDL cells is most affected. The cell type specific LL-37-induced attenuation of viability was not solely dependent on LL-37 ability to perforate the plasma membrane, since there was a prominent LDH release in all four cell types (Figure 4C and 4D), which may point to an intracellular mechanism that is responsible for the LL-37-evoked attenuation of cell viability. We further noted that PDL cells display a higher LL-37-induced LDH release than all other cells investigated. The strong LL-37-evoked decrease in cell viability was also reflected in reduced cell number and morphological changes, such as cell shrinkage and membrane blebbing, which were more pronounced in PDL cells compared to HDFa cells (Figure 5).

LL-37-induced cytotoxicity depends on the cellular expression level of p33

Based on these findings, we hypothesized that the differences in cell viability are due to the endogenous p33 expression levels in the cell lines tested. Therefore, we performed Western blotting for comparative analysis of the respective cellular p33 content in these cells (Figure 4E and 4F). HaCaT cells showed the highest p33 level, while lower levels were found in HDFa and MG63 cells. The lowest p33 content was detected in PDL cells. Additionally, we determined p33 mRNA levels in both MG63 and HaCaT cells revealing a 30% higher p33 mRNA level in HaCaT compared to MG63 cells (data not shown). Thus, HaCaT cells show higher expression of p33 than MG63 cells on both transcript and protein level.

Down-regulation of p33 by siRNA increases LL-37-induced cytotoxic effects

In order to demonstrate that p33 expression levels determine the sensitivity of cells to LL-37 treatment, we employed a siRNA approach to down-regulate p33 mRNA and protein. p33 siRNA transfection led to a decrease of p33 mRNA and protein levels both in MG63 and

HaCaT cells. As shown in Figure 6A and 6C, treatment with p33 siRNA reduced p33 mRNA and protein level in MG63 cells by 80 and 90%, respectively, compared to cells transfected with non-coding (NC) scramble and similar results were obtained when HaCaT cells were used (Figure 6B and 6D).

To compare the cytotoxic damage in p33 siRNA and non-coding construct transfected cells, we chose LL-37 concentrations which were below the EC_{50} values for each cell type (5 μM for MG63 and 9 μM HaCaT cells). Figure 7A shows that treatment with 1 and 4 μM LL-37 reduced MG63 cell viability, assessed by the MTT assay, by 30 and 50%, respectively, regardless whether p33 was present or knocked down in these cells (Figure 7A). In contrast, treatment of HaCaT cells with 6 and 8 μM LL-37 reduced viability significantly stronger in p33 siRNA-treated cells compared to cells transfected with a non-coding construct (Figure 7B). The p33 siRNA increased sensitivity to LL-37 in the HaCaT cells but not in MG63 cells probably because HaCaT cells contain about 6 times higher level of p33 than MG63 cells (Figure 4E), and therefore the absolute decrease in p33 evoked by p33 siRNA is greater in HaCaT compared to MG63 cells. Interestingly, the p33 knockdown in MG63 and HaCaT cells did not further affect the integrity of the plasma membrane, as LL-37-evoked LDH release was not increased in cells lacking p33 (Figure 7C and 7D). Our previous work has shown that treatment with p33 siRNA has no effect on LL-37-stimulated LDH release in MG63 cells [22]. Thus, these data suggest that the intracellular level of p33 regulates cell viability.

Over-expression of p33 antagonizes LL-37-evoked cytotoxicity

Having shown that removal of p33 enhances the cytotoxic effects of LL-37, we next wished to analyze whether p33 up-regulation renders cells more resistant to LL-37. To this end, HeLa cells were employed because their transfection efficiency was significantly higher than that of MG63 and HaCaT cells. Notably, HeLa cells show similar p33 expression levels for both mRNA and protein compared to MG63 cells (data not shown). In cells transiently transfected with pcDNA 3.1-p33 vector, p33 mRNA level was increased by about 200 times compared to cells transfected only with pcDNA 3.1 vector as control (Figure 8A). Additional Western blot analysis revealed that the p33 protein level was increased about 2 times after transfection (Figure 8B). The increase in p33 rendered the cells completely resistant against an LL-37 attack, as depicted in Figure 8C. The data show that cell viability in HeLa cells over-expressing p33 was not affected by 4 μM LL-37, while the same concentration of LL-37 (4 μM) reduced cell viability by about 30% in control cells (Figure 8C). As before, this effect seems to be only evoked by the intracellular p33, since LL-37 (4 μM) triggered a similar LDH release in p33 over-expressing and control cells (Figure 8D). Thus, over-expression of p33 completely abolished the LL-37-induced attenuation of cell viability but showed no effect on LDH release.

p33 interacts with LL-37

As our results imply that the toxic effects of intracellular LL-37 are neutralized by p33, we next wished to demonstrate that the two proteins bind to each other upon internalization of LL-37. These experiments were performed with HaCaT cells since they show high expression of endogenous p33 (Figure 4E). The cells were first incubated with LL-37 (10 μM) for 10 min and after a lysis step the interaction between p33 and LL-37 was investigated by co-immunoprecipitation. Immunoblot (dot blot) of the precipitates demonstrates interaction of the two proteins (Figure 9A) suggesting that LL-37 is targeted by p33 and this leads to a down-regulation of the deleterious effects of LL-37. In order to provide further evidence that

intracellular p33 binds LL-37, we treated HaCaT and HeLa cells with LL-37 (10 μM) for 10 min, then performed sub-cellular fractionation, and determined the interaction between intracellular p33 and LL-37 by co-immunoprecipitation in cytosolic fractions of HaCaT and HeLa cells. Dot blot showed interaction of p33 with LL-37 in a cytosolic fraction of HaCaT and HeLa cells (Figure 9A and B). Moreover, we demonstrate stronger interaction between p33 and LL-37 in a cytosolic fraction of HeLa cells transfected with the pcDNA 3.1-p33 vector compared to cells transfected with the control vector (Figure 9B). The interaction between p33 and LL-37 was about two times higher in p33 over-expressing HeLa cells compared to control cells assessed by densitometry (205±10% in p33 over-expressing cells vs. 100±6% in control cells, $P<0.001$, $n=3$ in both groups). These data support our working hypothesis that intracellular p33 is responsible for down-regulating the deleterious activity of LL-37.

LL-37 up-regulates p33 expression in MG63 cells

In the last series of experiments we were wondering whether p33 up-regulation constitutes a host defense mechanism that makes cells less susceptible to an LL-37 attack under pathological conditions. Figure 10 shows that treatment with 4 μM LL-37 for 48 h increased MG63 p33 protein expression by about 50%, while LL-37 (8 μM) had no effect on HaCaT p33 protein expression. The LL-37-induced up-regulation of MG63 p33 protein expression was confirmed on the mRNA level (data not shown). Treatment with a higher concentration of LL-37 (8 μM) increased MG63 p33 protein level by 55% (100 ± 11% in control cells vs. 155 ± 13% in LL-37-treated cells, $p<0.01$, $n=5$ for both groups). In contrast, incubation with the well-known pro-apoptotic compound staurosporine (0.5, 1 and 1.5 μM) for 48 h had no effect on MG63 p33 protein expression, suggesting that LL-37-evoked up-regulation of p33 is specific for LL-37 and not secondary to the pro-apoptotic process (data not shown).

DISCUSSION

Modulation of inflammatory reactions in infectious diseases is tightly regulated and their disturbance often decides about the fate of disease progression [33]. Notably, pattern recognition receptors are key players in these processes since they are among the first sentinels that sense the invading pathogen [34]. Apart from microorganism-derived ligands, pattern recognition receptors can be activated by danger signals. These are often host factors mobilized under disease conditions that are up-regulated or released upon an inflammatory signal [35].

In 2010, Into and colleagues reported for the first time that LL-37 is a danger-associated molecular pattern (DAMP) peptide, as it modulates the activity of toll-like receptors and triggers the mobilization of inflammatory and chemotactic mediators, such as interleukin-6 (IL-6), IL-8, and CXCL10, respectively [36]. Interestingly, due to its amphiphilic nature caused by the hydrophobic and hydrophilic residues of LL-37, the peptide is able to penetrate eukaryotic plasma membranes and subsequently enter the cytosol. Intracellularly, LL-37 not only exerts its antimicrobial activity by killing invaded microorganisms [37], but it can also block inflammasome formation by binding to cytosolic DNA [38]. However, not much is known of how the activity of cytosolic LL-37 is regulated.

The data presented in this study suggest a critical role for internalized LL-37, as the intracellular pool of the peptide is also crucial for impairing cell viability. We further find that its cytotoxic activity is regulated by p33, a protein also known as gC1q receptor or p32.

Importantly, p33 and LL-37 show direct intracellular interaction demonstrated by co-immunoprecipitation. p33 was originally described as a receptor for the globular part of complement factor C1q [26], but subsequent analysis revealed that p33 possesses a canonical N-terminal specific localization sequence that targets the protein to the mitochondria [39]. However, apart from the cell membrane and mitochondria, also other cellular locations such as the nucleus have been described for p33 [40]. A multi-subcellular distribution of p33 was also observed in our experiments. Though a big p33 pool was localized to the mitochondria, the protein was also found at the plasma membrane and within the cytosol. The relative importance of mitochondrial, plasma membrane and cytosolic p33 for the binding of LL-37 may indeed vary between different cell types. We cannot completely rule out additional protective mechanisms, besides p33, explaining the cell type-dependent differences in LL-37 sensitivity. The high expression level of p33 in HaCaT cells compared to other human cell types observed in the present study may reflect that skin keratinocytes represent an outer barrier exposed to high LL-37 concentrations.

It is worth mentioning that recent work has pointed to a role of p33 in regulating cellular fitness. For instance, Xiao and co-workers published a study in 2014 showing that mitochondrial p33 is pro-apoptotic and regulates mitochondrial calcium up-take [41], whereas Watthanasurorot and collaborators employ an arthropod model to demonstrate that binding of cytosolic p33 to calreticulin protects cells from dying [42]. While the molecular mechanisms are not completely understood, it appears that shuttling of p33 between the cytosol and mitochondria or the nucleus is essential in these processes [42, 43]. Dual or multifold intracellular targeting of proteins with specific localization sequences is an emerging field of research [44, 45] and several mechanisms have been proposed to explain this phenomenon. These include, for instance, different or several translation products, multiple mRNAs or membrane permeabilization. However, so far the subcellular distribution of p33 remains unexplained. Interestingly, in our experiments cytosolic over-expression revealed that p33 counteracts LL-37 induced cell death, but not cell perforation. This suggests that intracellular p33, either the mitochondrial or the cytosolic fraction or both, binds and inactivates LL-37.

Considering the capability of LL-37 to modulate Toll-like receptor activity and evoke inflammatory reactions, intracellular damage caused by the peptide would be counterproductive and impair the cellular response. Therefore, cells have to rely on intracellular defense mechanisms that prevent cellular damage evoked by cytosolic LL-37. Bearing in mind that mitochondria are evolutionary of prokaryotic origin, it seems plausible that localization of p33 to this organelle prevents further damage by internalized HDPs with antimicrobial activities. Our data therefore point to an important role of p33 in preventing intracellular cytotoxic effects of LL-37, or other HDPs, without influencing the antimicrobial and inflammatory activities of these peptides.

ACKNOWLEDGEMENTS

The authors wish to thank Dr. Daniel Nebel for providing the human periodontal ligament fibroblasts, Dr. Uta Rabenhorst for providing the GFP-vector, and Dr. Ole Sørensen for advice on transfection protocols.

AUTHOR CONTRIBUTION

Daniel Svensson designed, planned and preformed the experiments with the exception of immunogold electron microscopy and preparation of the p33 plasmid, and wrote the paper. Laura Wilk prepared the plasmid DNA, preformed experiments on p33 overexpression and wrote the paper. Matthias Mörgelin preformed immunogold electron microscopy. Heiko Herwald designed the study and wrote the paper. Bengt-Olof Nilsson designed the study and wrote the paper.

FUNDING

This study was supported by grants from the Swedish Research Council [grant number 2003-7605 (to B.O.N.) and grant number SB12–0019 (to H.H.)], the Swedish Dental Society (to B.O.N.), the Southern Region within the Swedish Dental Association (to B.O.N.), the Greta and Johan Kock Foundation (to B.O.N.), the Swedish Foundation for Strategic Research [grant number K2014–56X-13413–15–3 (to H.H.)], the Ragnar Söderberg Foundation (to H.H.), the Knut and Alice Wallenberg Foundation [grant number KAW 2011.0037 (to H.H.)], the Alfred Österlund Foundation (to H.H.), and the Medical Faculty, Lund University.

REFERENCES

1. Mansour, S. C., Pena, O. M. and Hancock, R. E. (2014) Host defense peptides: front-line immunomodulators. Trends. Immunol. **35**, 443-450
2. Choi, K. Y., Chow, L. N. and Mookherjee, N. (2012) Cationic host defence peptides: multifaceted role in immune modulation and inflammation. J. Innate Immun. **4**, 361-370
3. Yeung, A. T., Gellatly, S. L. and Hancock, R. E. (2011) Multifunctional cationic host defence peptides and their clinical applications. Cell. Mol. Life Sci. **68**, 2161-2176
4. van der Does, A. M., Joosten, S. A., Vroomans, E., Bogaards, S. J., van Meijgaarden, K. E., Ottenhoff, T. H., van Dissel, J. T. and Nibbering, P. H. (2012) The antimicrobial peptide hLF1-11 drives monocyte-dendritic cell differentiation toward dendritic cells that promote antifungal responses and enhance Th17 polarization. J. Innate Immun. **4**, 284-292
5. Burton, M. F. and Steel, P. G. (2009) The chemistry and biology of LL-37. Nat. Prod. Rep. **26**, 1572-1584
6. Turner, J., Cho, Y., Dinh, N. N., Waring, A. J. and Lehrer, R. I. (1998) Activities of LL-37, a cathelin-associated antimicrobial peptide of human neutrophils. Antimicrob. Agents Chemother. **42**, 2206-2214
7. Nizet, V., Ohtake, T., Lauth, X., Trowbridge, J., Rudisill, J., Dorschner, R. A., Pestonjamasp, V., Piraino, J., Huttner, K. and Gallo, R. L. (2001) Innate antimicrobial peptide protects the skin from invasive bacterial infection. Nature **414**, 454-457
8. Larrick, J. W., Hirata, M., Balint, R. F., Lee, J., Zhong, J. and Wright, S. C. (1995) Human CAP18: a novel antimicrobial lipopolysaccharide–binding protein. Infect. Immun. **63**, 1291-1297
9. Kahlenberg, J. M. and Kaplan, M. J. (2013) Little peptide, big effects: the role of LL-37 in inflammation and autoimmune disease. J. Immunol. **191**, 4895-4901
10. Säll, J., Carlsson, M., Gidlöf, O., Holm, A., Humlén, J., Öhman, J., Svensson, D., Nilsson, B. O. and Jönsson, D. (2013) The antimicrobial peptide LL-37 alters human osteoblast Ca^{2+} handling and induces Ca^{2+}-independent apoptosis. J. Innate Immun. **5**, 290-300
11. Ciornei, C. D., Tapper, H., Bjartell, A., Sternby, N. H. and Bodelsson, M. (2006) Human antimicrobial peptide LL-37 is present in atherosclerotic plaques and induces death of vascular smooth muscle cells: a laboratory study. BMC Cardiovasc. Disord. **6**, 49
12. Jönsson, D. and Nilsson, B. O. (2012) The antimicrobial peptide LL-37 is anti-inflammatory and pro-apoptotic in human periodontal ligament cells. J. Periodont. Res. **47**, 330-335
13. Zhang, Z., Cherryholmes, G. and Shively, J. E. (2008) Neutrophil secondary necrosis is induced by LL-37 derived from cathelicidin. J. Leukoc. Biol. **84**, 780-788

14. Barlow, P. G., Beaumont, P. E., Cosseau, C., Mackellar, A., Wilkinson, T. S., Hancock, R. E., Haslett, C., Govan, J. R., Simpson, A. J. and Davidson, D. J. (2010) The human cathelicidin LL-37 preferentially promotes apoptosis of infected airway epithelium. Am. J. Respir. Cell. Mol. Biol. **43**, 692-702
15. Mader, J. S., Ewen, C., Hancock, R. E. and Bleackley, R. C. (2011) The human cathelicidin, LL-37, induces granzyme-mediated apoptosis in regulatory T cells. J. Immunother. **34**, 229-235
16. Ong, P. Y., Ohtake, T., Brandt, C., Strickland, I., Boguniewicz, M., Ganz, T., Gallo, R. L. and Leung, D. Y. (2002) Endogenous antimicrobial peptides and skin infections in atopic dermatitis. N. Engl. J. Med. **347**, 1151-1160
17. Yamasaki, K., Di Nardo, A., Bardan, A., Murakami, M., Ohtake, T., Coda A., Dorschner, R. A., Bonnart, C., Descargues, P., Hovnanian, A., Morhenn, V. B. and Gallo, R. L. (2007) Increased serine protease activity and cathelicidin promotes skin inflammation in rosacea. Nat. Med. **13**, 975-980
18. Schauber, J., Rieger, D., Weiler, F., Wehkamp, J., Eck, M., Fellermann, K., Scheppach, W., Gallo, R. L. and Stange, E. F. (2006) Heterogenous expression of human cathelicidin hCAP18/LL-37 in inflammatory bowel diseases. Eur. J. Gastroenterol. Hepatol. **18**, 615-621
19. Türkoğlu, O., Emingil, G., Kutukculer, N. and Atilla, G. (2009) Gingival crevicular fluid levels of cathelicidin LL-37 and interleukin-18 in patients with chronic periodontitis. J. Periodontol. **80**, 969-976
20. Herwald, H., Dedio, J., Kellner, R., Loos, M. and Müller-Esterl, W. (1996) Isolation and characterization of the kininogen-binding protein p33 from endothelial cells. Identity with the gC1q receptor. J. Biol. Chem. **271**, 13040-13047
21. Peerschke, E. I., Murphy, T. K. and Ghebrehiwet, B. (2003) Activation-dependent surface expression of gC1qR/p33 on human platelets. Thromb. Haemost. **89**, 331-339
22. Svensson, D., Westman, J., Wickström, C., Jönsson, D., Herwald, H. and Nilsson, B. O. (2015) Human endogenous peptide p33 inhibits detrimental effects of LL-37 on osteoblast viability. J. Periodont. Res. **50**, 80-88
23. Ghebrehiwet, B. and Peerschke, E. I. (2004) cC1q-R (calreticulin) and gC1q-R/p33: ubiquitously expressed multi-ligand binding cellular proteins involved in inflammation and infection. Mol. Immunol. **41**, 173-183
24. Peerschke, E. I. and Ghebrehiwet, B. (2014) cC1qR/CR and gC1qR/p33: observations in cancer. Mol. Immunol. **61**, 100-109
25. Jiang, J., Zhang, Y., Krainer, A. R. and Xu, R. M. (1999) Crystal structure of human p32, a doughnut-shaped acidic mitochondrial matrix protein. Proc. Natl. Acad. Sci. USA **96**, 3572-3577
26. Ghebrehiwet, B., Lim, B. L., Peerschke, E. I., Willis, A. C. and Reid, K. B. (1994) Isolation, cDNA cloning, and overexpression of a 33-kD cell surface glycoprotein that binds to the globular "heads" of C1q. J. Exp. Med. **179**, 1809-1821
27. Westman, J., Hansen, F. C., Olin, A. I., Mörgelin, M., Schmidtchen, A. and Herwald, H. (2013) p33 (gC1q receptor) prevents cell damage by blocking the cytolytic activity of antimicrobial peptides. J. Immunol. **191**, 5714-5721
28. Nebel, D., Jönsson, D., Norderyd, O., Bratthall, G. and Nilsson, B. O. (2010) Differential regulation of chemokine expression by estrogen in human periodontal ligament cells. J. Periodont. Res. **45**, 796-802
29. Carmichael, J., De Graff, W. G., Gazdar, A. F., Minna, J. D. and Mitchell, J. B. (1987) Evaluation of a tetrazolium-based semiautomated colorimetric assay: assessment of chemosensitivity testing. Cancer Res. **47**, 936-942
30. Stirling, J. W. and Graff, P. S. (1995) Antigen unmasking for immunoelectron microscopy: labeling is improved by treating with sodium ethoxide or sodium metaperiodate then heating on retrieval medium. J. Histochem. Cytochem. **43**, 115-123
31. Pfaffl, M. W. (2001) A new mathematical model for relative quantification in real-time RT-PCR. Nucleic Acids Res. **29**, e45
32. Dedio, J. and Müller-Esterl, W. (1996) Kininogen binding protein p33/gC1qR is localized in the vesicular fraction of endothelial cells. FEBS Letters **399**, 255-258.

33. Hotchkiss, R. S., Coopersmith, C. M., McDunn, J. E. and Ferguson, T. A. (2009) The sepsis seesaw: tilting toward immunosuppression. Nat. Med. **15**, 496-497
34. Kawai, T. and Akira, S. (2010) The role of pattern-recognition receptors in innate immunity: update on Toll-like receptors. Nat. Immunol. **11**, 373-384
35. Schaefer, L. (2014) Complexity of danger: the diverse nature of damage-associated molecular patterns. J. Biol. Chem. **289**, 35237-35245
36. Into, T., Inomata, M., Shibata, K. and Murakami, Y. (2010) Effect of the antimicrobial peptide LL-37 on Toll-like receptors 2-, 3- and 4-triggered expression of IL-6, IL-8 and CXCL10 in human gingival fibroblasts. Cell. Immunol. **264**, 104-109
37. Noore, J., Noore, A. and Li, B. (2013) Cationic antimicrobial peptide LL-37 is effective against both extra- and intracellular Staphylococcus aureus. Antimicrob. Agents Chemother. **57**, 1283-1290
38. Dombrowski, Y., Peric, M., Koglin, S., Kammerbauer, C., Goss, C., Anz, D., Simanski, M., Glaser, R., Harder, J., Hornung, V., Gallo, R. L., Ruzicka, T., Besch, R. and Schauber, J. (2011) Cytosolic DNA triggers inflammasome activation in keratinocytes in psoriatic lesions. Sci. Transl. Med. **3**, 82ra38
39. Dedio, J., Jahnen-Dechent, W., Bachmann, M. and Muller-Esterl, W. (1998) The multiligand-binding protein gC1qR, putative C1q receptor, is a mitochondrial protein. J. Immunol. **160**, 3534-3542
40. Ghebrehiwet, B., Lim, B. L., Kumar, R., Feng, X. and Peerschke, E. I. (2001) gC1q-R/p33, a member of a new class of multifunctional and multicompartmental cellular proteins, is involved in inflammation and infection. Immunol. Rev. **180**, 65-77
41. Xiao, K., Chen, P. and Chang, D. C. (2014) The VTLISFG motif in the BH1 domain plays a significant role in regulating the degradation of Mcl-1. FEBS Open Bio. **4**, 147-152
42. Watthanasurorot, A., Jiravanichpaisal, P., Soderhall, K. and Soderhall, I. (2013) A calreticulin/gC1qR complex prevents cells from dying: a conserved mechanism from arthropods to humans. J. Mol. Cell. Biol. **5**, 120-131
43. Kamal, A. and Datta, K. (2006) Upregulation of hyaluronan binding protein 1 (HABP1/p32/gC1qR) is associated with Cisplatin induced apoptosis. Apoptosis **11**, 861-874
44. Karniely, S. and Pines, O. (2005) Single translation--dual destination: mechanisms of dual protein targeting in eukaryotes. EMBO Rep. **6**, 420-425
45. Yogev, O. and Pines, O. (2011) Dual targeting of mitochondrial proteins: mechanism, regulation and function. Biochim. Biophys. Acta **1808**, 1012-1020

FIGURE LEGENDS

FIGURE 1. **p33 is localized to the mitochondria in human HaCaT keratinocytes.**
(A) Laser scanning confocal images of human osteoblast-like MG63 cells stained with p33 antibody (green). (**B**) p33 immunoreactivity in one cell indicated in panel (A) at higher magnification. **(C-D)** HaCaT cells double-stained for p33 immunoreactivity (C, green) and MitoTracker (D, red). **(E)** Overlay of p33 immunoreactive signal (green) and MitoTracker staining (red) represented by yellow color. Scale bars = 10 μm.

FIGURE 2. **Sub-cellular distribution of p33 and down-regulation by p33 siRNA in MG63 and HaCaT cells.**
(A-D) Immunogold electron microscopy of MG63 cells (A, B) and human HaCaT keratinocytes (C, D). MG63 and HaCaT control cells (A, C) and after treatment with p33 siRNA (B, D) were fixed and thin-sectioned followed by immune detection with p33 antibody and a secondary gold-labeled antibody. Scale bars = 250 nm.

FIGURE 3. **Sub-cellular distribution of p33 in HDFa and PDL cells.**
(A-B) HDFa (A) and PDL cells (B) were fixed and thin-sectioned for immunogold electron microscopy. Immune detection was performed with a p33 antibody and a secondary gold-labeled antibody. Scale bar = 250 nm.

FIGURE 4. **Correlation between reduced cell viability for LL-37 treated human cell lines and cellular p33 level.**
(A-B) MG63 and HaCaT cells (A) or PDL and HDFa cells (B) were incubated with LL-37 for 3 h and cell viability was assessed by the MTT assay. The dotted line in panel B represents the dose-response curve for MG63 cells as a reference. **(C-D)** MG63 and HaCaT cells (C) or PDL and HDFa cells (D) were treated with LL-37 for 30 min and LDH release was determined. The dotted line in panel D represents the dose-response curve for MG63 cells as a reference. **(E-F)** MG63 and HaCaT cells (E) or PDL and HDFa cells (F) were lysed and analyzed by Western blotting using a p33 antibody. Immunostaining against GAPDH served as internal control (lower part). Relative p33 concentration was quantified by densitometry and is shown in the upper part. The open column in panel F represents MG63 p33 expression level for reference. MW in panel E = Molecular Weight standard. Summarized data are presented as means ± SEM of 4-6 observations in each experimental group. *, ** and *** represent $P<0.05$, $P<0.01$ and $P<0.001$, respectively.

FIGURE 5. **Morphological analysis of LL-37-treated PDL and HDFa cells.**
(A-D) Light microscopic analysis of PDL (A, C) and HDFa (B, D) fibroblasts before (A, B) and after (C, D) treatment with 8 μM LL-37 for 24 h. Scale bar = 20 μm.

FIGURE 6. **p33 siRNA reduces p33 mRNA and protein expression levels.**
(A-D) MG63 (A, C) and HaCaT (B, D) cells were treated with p33 siRNA. Control cells were transfected with a non-coding construct (NC). **(A-B)** p33 mRNA levels determined by quantitative real-time RT-PCR. **(C-D)** Western blot analysis of p33 protein levels. A densitometric analysis showing the relative p33 concentration is given in the upper part. Immunostaining against Hsp90 was used as internal control. Summarized data are presented as means ± SEM (error bars) of 6 observations in each experimental group. *, ** and *** represent $P<0.05$, $P<0.01$ and $P<0.001$, respectively.

FIGURE 7. **Treatment with p33 siRNA enhances sensitivity to LL-37 in HaCaT cells.**

(A-D) MG63 (A, C) and HaCaT (B, D) cells were transfected with p33 siRNA or non-coding construct (NC). Control cells were not treated with LL-37. Transfected cells were treated with 1 and 4 μM LL-37 for MG63 cells or 6 and 8 μM LL-37 for HaCaT cells, and cell viability (A, B) or LDH release (C, D) was assessed after 3 h or 30 min, respectively (ns = non-significant). The concentrations of LL-37 used for MG63 and HaCaT cells were below their respective EC_{50} value (MG63 = 5 μM, HaCaT = 9 μM). Data are presented as means ± SEM of 6 observations in each experimental group. ** represents $P<0.01$.

FIGURE 8. **LL-37 has no effect on cell viability in HeLa cells over-expressing p33.**
(A-D) HeLa cells were transiently transfected with pcDNA 3.1-p33 vector or pcDNA 3.1 vector as control for 24 h. For these experiments, HeLa cells were employed because their transfection efficiency was significantly higher than that of MG63 and HaCaT cells. **(A-B)** Up-regulation of p33 mRNA assessed by quantitative real-time RT-PCR (A) and Western blotting for p33 protein expression using Hsp90 as house-keeping protein (B). **(C)** Cell viability of transfected cells, assessed by the MTT assay, after treatment with LL-37 (4 μM) for 3 h compared to untreated control cells (ns = non-significant). **(D)** LDH release from control cells and from cells treated with LL-37 (4 μM) for 30 min. Summarized data are presented as means ± SEM of 6 observations in each experimental group. ** and *** represent $P<0.05$, $P<0.01$ and $P<0.001$, respectively.

FIGURE 9. **Co-immunoprecipitation shows interaction between p33 and LL-37.**
(A) Co-immunoprecipitation (IP) of p33 and LL-37 in HaCaT cells incubated with LL-37 (10 μM) for 10 minutes. Cells were then lysed and LL-37-p33 complexes were immuno-precipitated with antibodies against p33. LL-37 immunoreactivity was detected by dot blot. Dot 1 and 2 represent immunoprecipitate without and with p33 antibody, respectively. Dot 3 shows synthesized LL-37 (100 ng) as positive control. Dot 4 visualizes the cell lysate used for the IP. Dot 5 shows SDS sample buffer as background control. Dot 6 represents immunoprecipitate with p33 antibody in a cytosolic fraction. **(B)** IP of p33 and LL-37 in cytosolic fractions of HeLa cells transfected with either pcDNA 3.1-p33 vector (dot 2) or pcDNA 3.1 vector as control (dot 1) for 24 h.

FIGURE 10. **LL-37 triggers p33 protein expression in MG63 cells.**
(A-B) MG63 (A) and HaCaT cells (B) were treated with 4 μM and 8 μM LL-37 for 48 h, respectively (ns = non-significant). Untreated cells served as control. p33 protein levels were analyzed by Western blotting and relative protein concentration determined by densitometry (upper part). Immunostaining against GAPDH served as internal control. Summarized data are presented as means ± SEM of 6 observations in each experimental group. *** represents $P<0.001$.

Figure 1

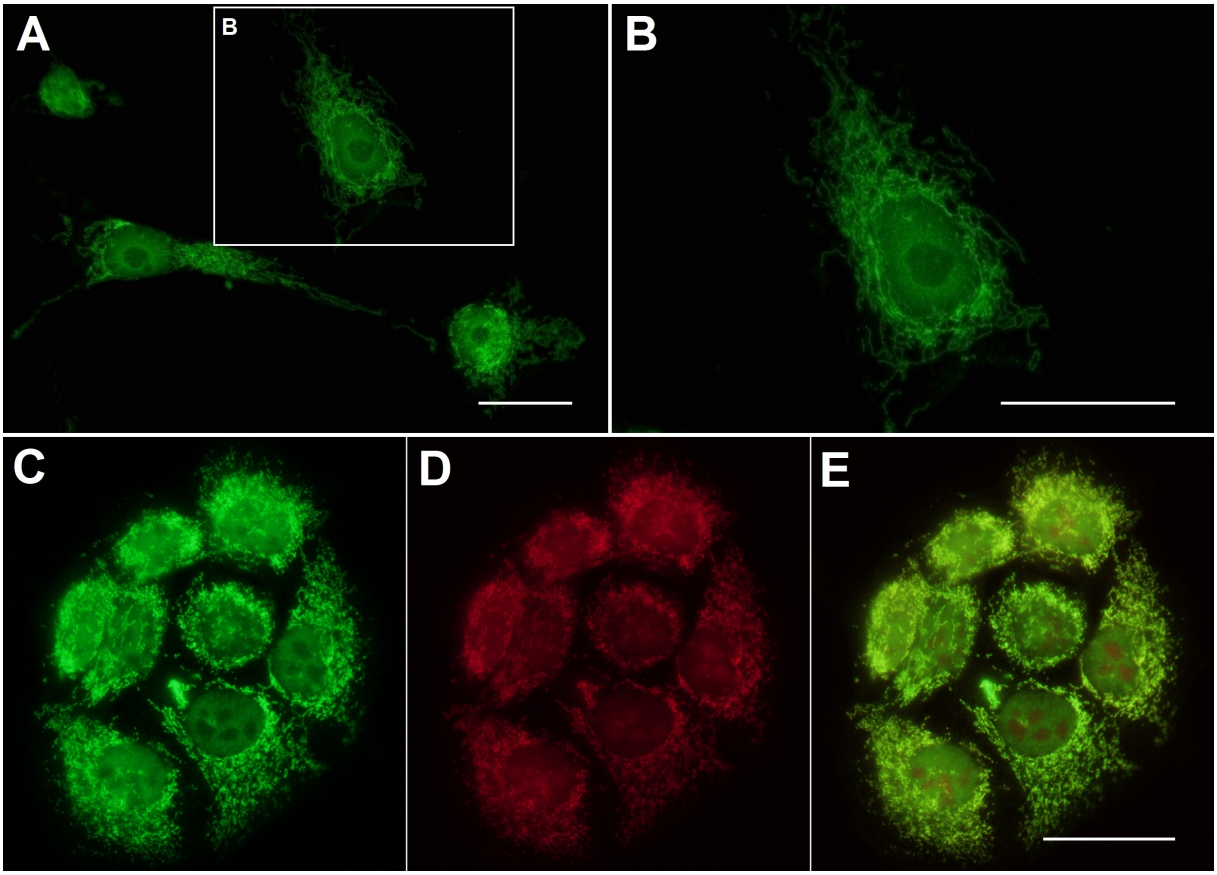

Figure 2

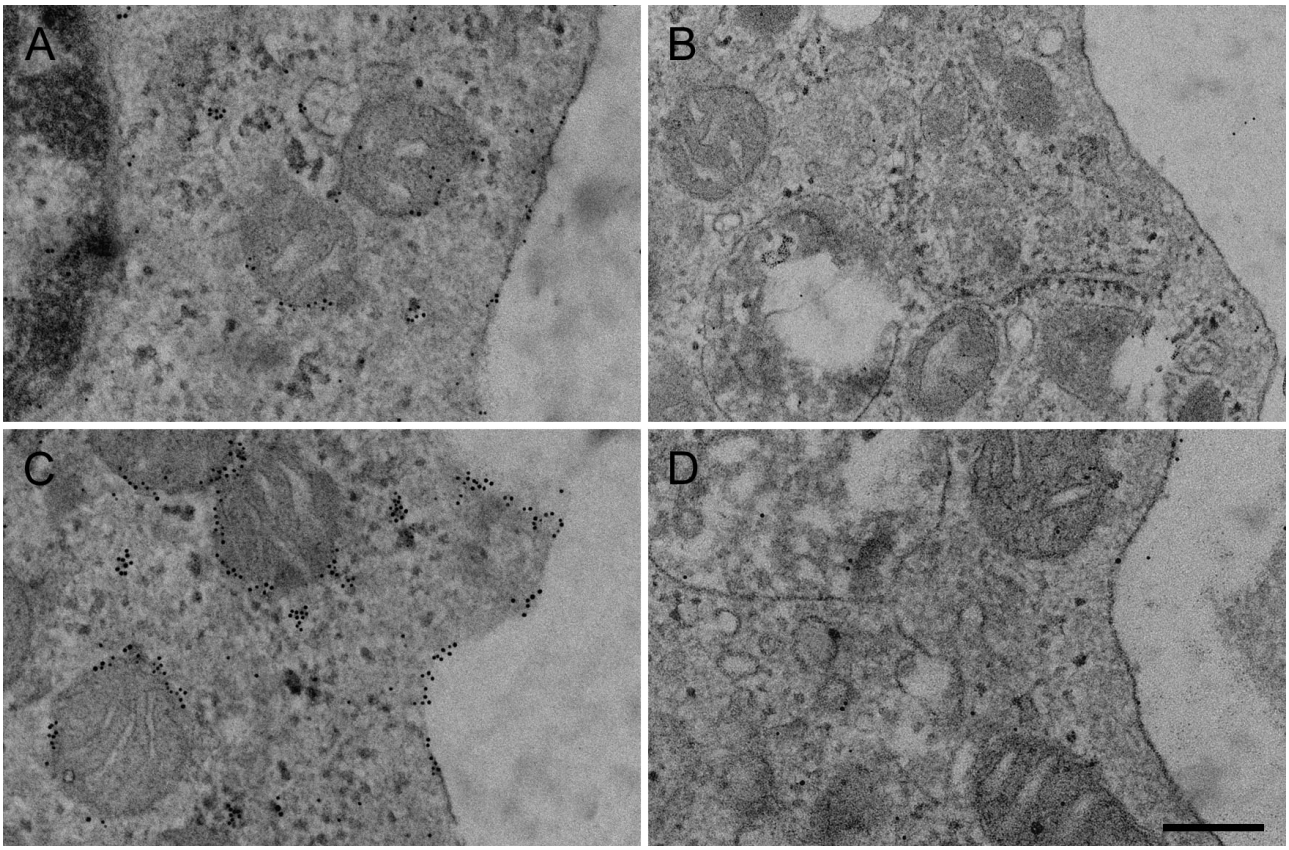

Figure 3

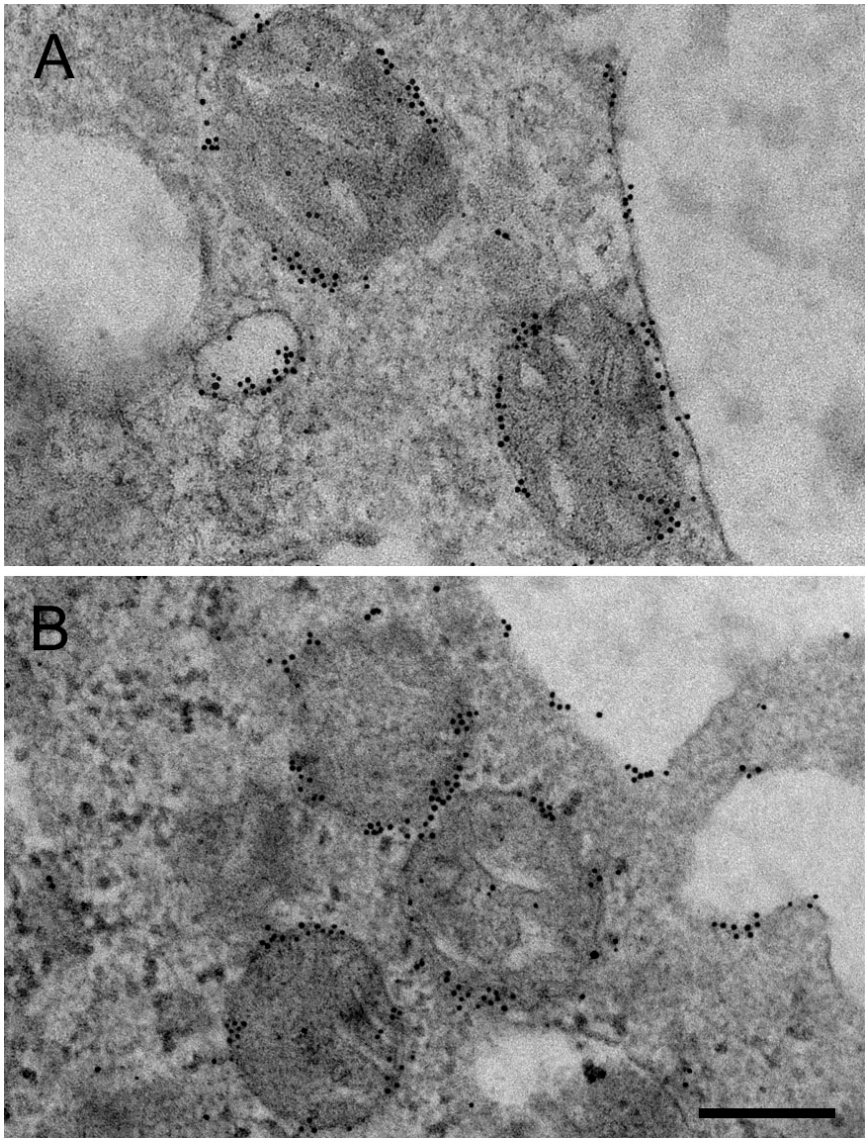

Figure 4

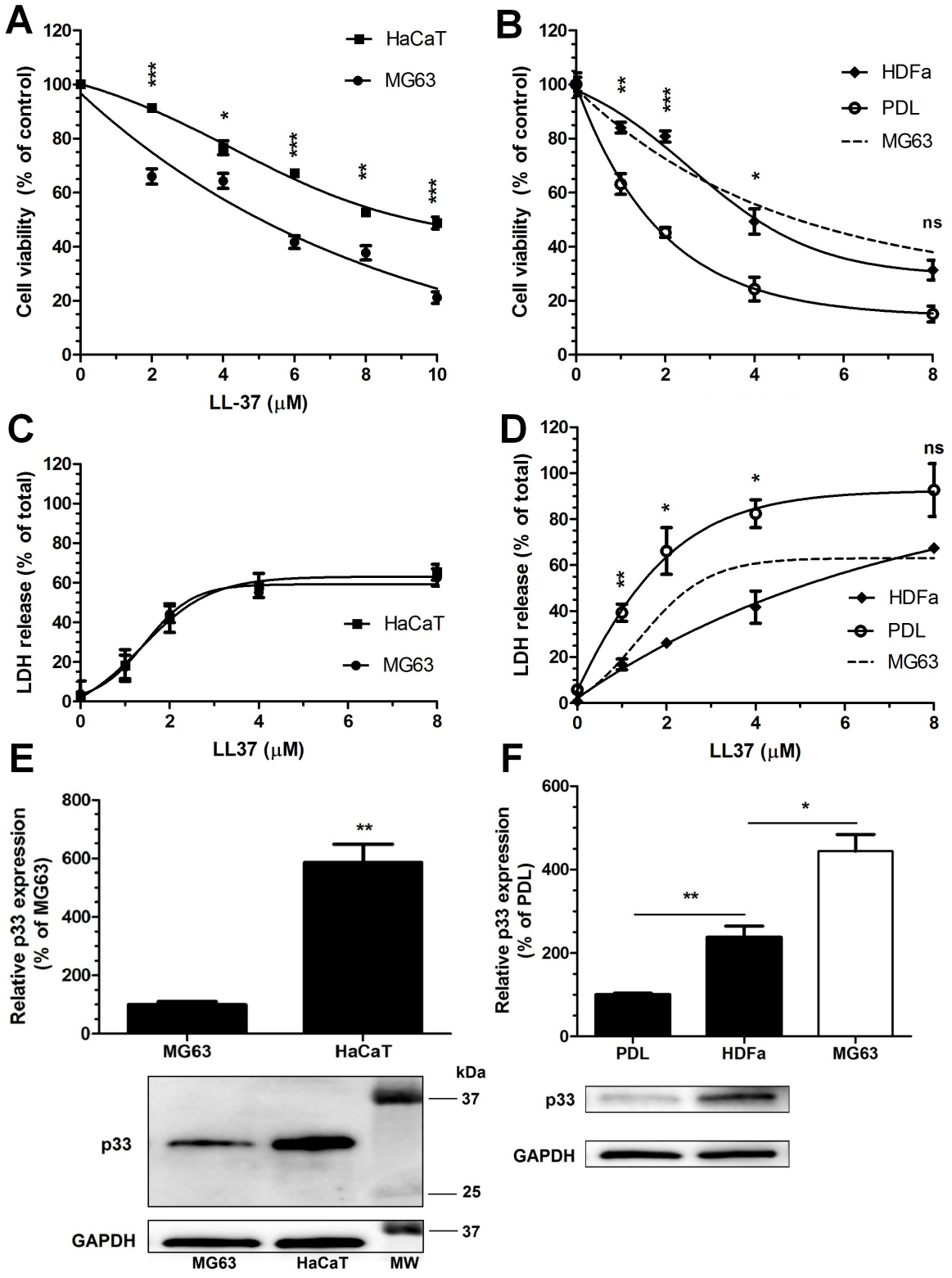
A
Cell viability (% of control)
LL-37 (μM)
HaCaT
MG63
B
Cell viability (% of control)
HDFa
PDL
MG63
ns
C
LDH release (% of total)
LL37 (μM)
HaCaT
MG63
D
LDH release (% of total)
LL37 (μM)
ns
HDFa
PDL
MG63
E
Relative p33 expression (% of MG63)
MG63
HaCaT
kDa
p33
37
25
GAPDH
37
MG63
HaCaT
MW
F
Relative p33 expression (% of PDL)
PDL
HDFa
MG63
p33
GAPDH

Figure 5

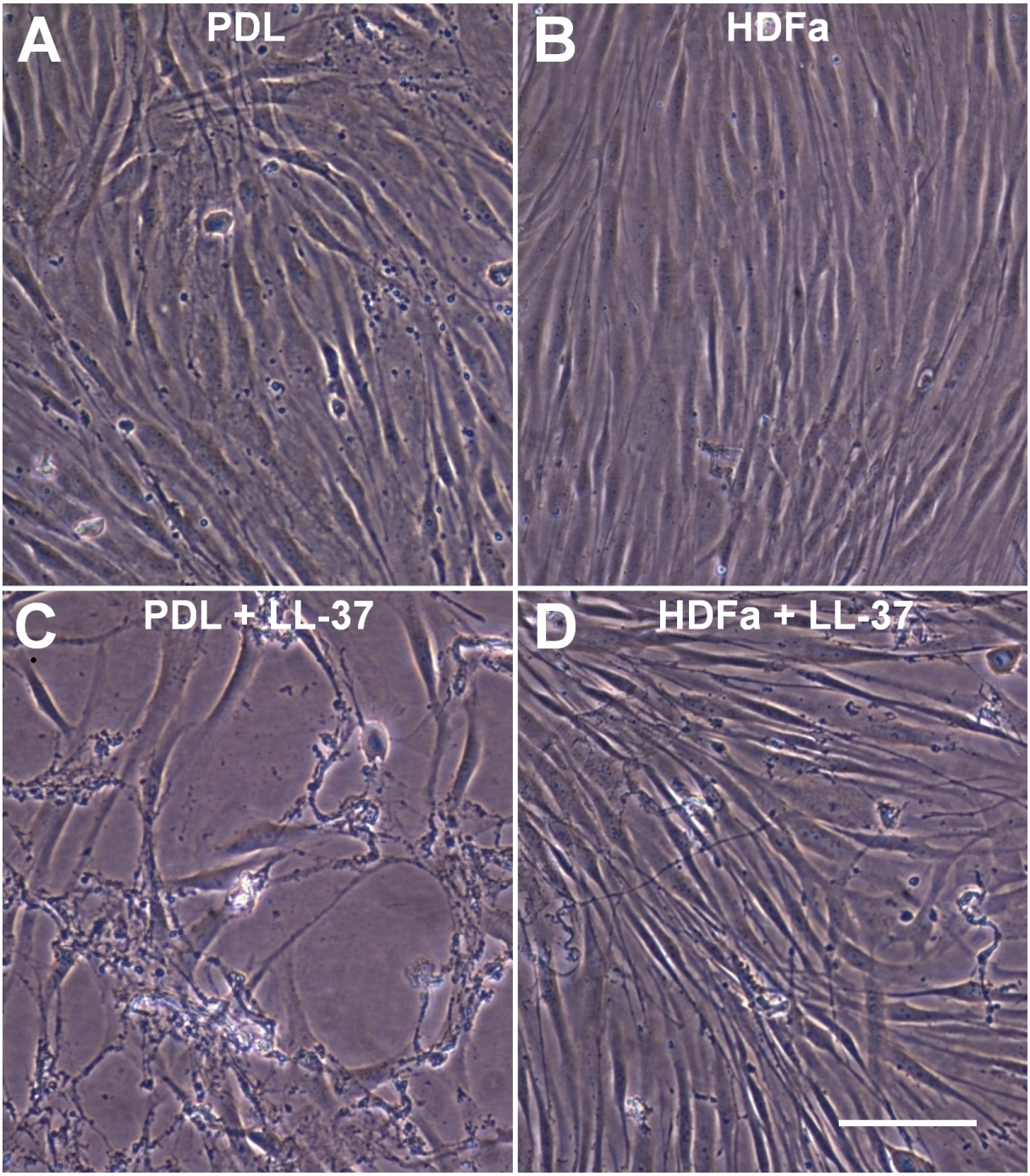

Figure 6

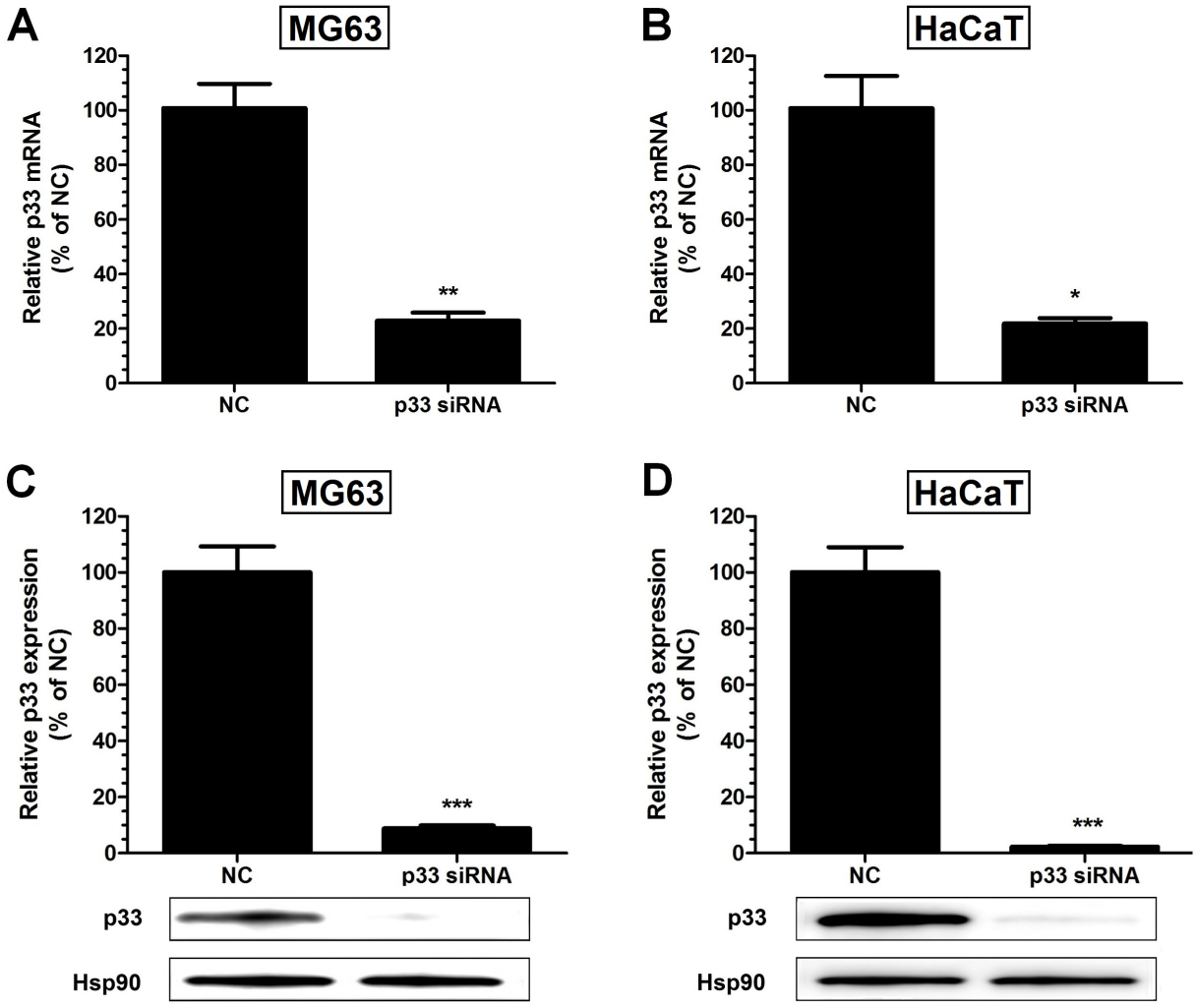
A
MG63
Relative p33 mRNA (% of NC)
120
100
80
60
40
20
0
**
NC
p33 siRNA
B
HaCaT
Relative p33 mRNA (% of NC)
*
NC
p33 siRNA
C
MG63
Relative p33 expression (% of NC)
***
NC
p33 siRNA
p33
Hsp90
D
HaCaT
Relative p33 expression (% of NC)
***
NC
p33 siRNA
p33
Hsp90

Figure 7

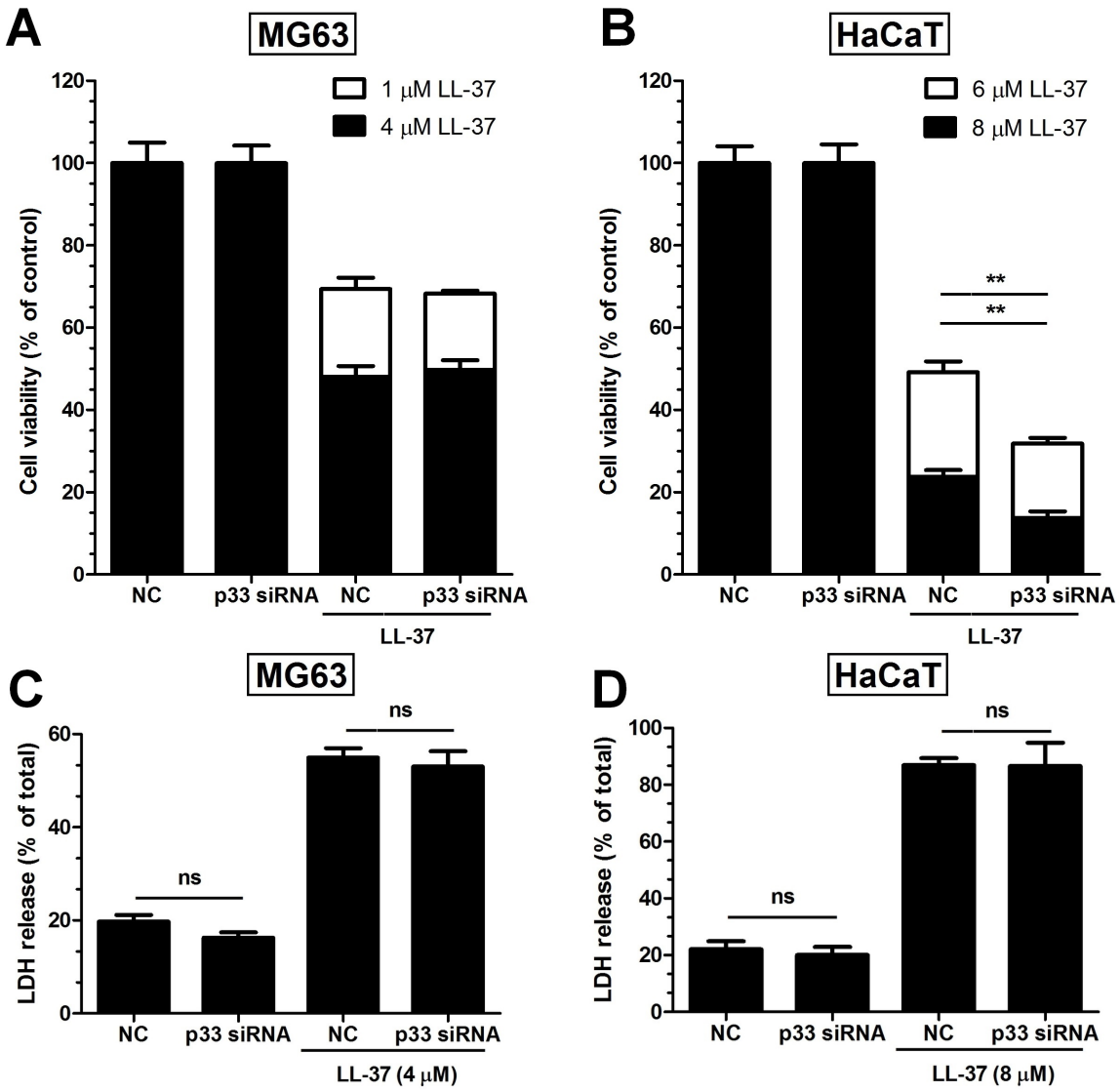
A
MG63
1 μM LL-37
4 μM LL-37
Cell viability (% of control)
120
100
80
60
40
20
0
NC
p33 siRNA
NC
p33 siRNA
LL-37
B
HaCaT
6 μM LL-37
8 μM LL-37
Cell viability (% of control)
**
**
NC
p33 siRNA
NC
p33 siRNA
LL-37
C
MG63
LDH release (% of total)
60
40
20
0
ns
ns
NC
p33 siRNA
NC
p33 siRNA
LL-37 (4 μM)
D
HaCaT
LDH release (% of total)
100
80
60
40
20
0
ns
ns
NC
p33 siRNA
NC
p33 siRNA
LL-37 (8 μM)

Figure 8

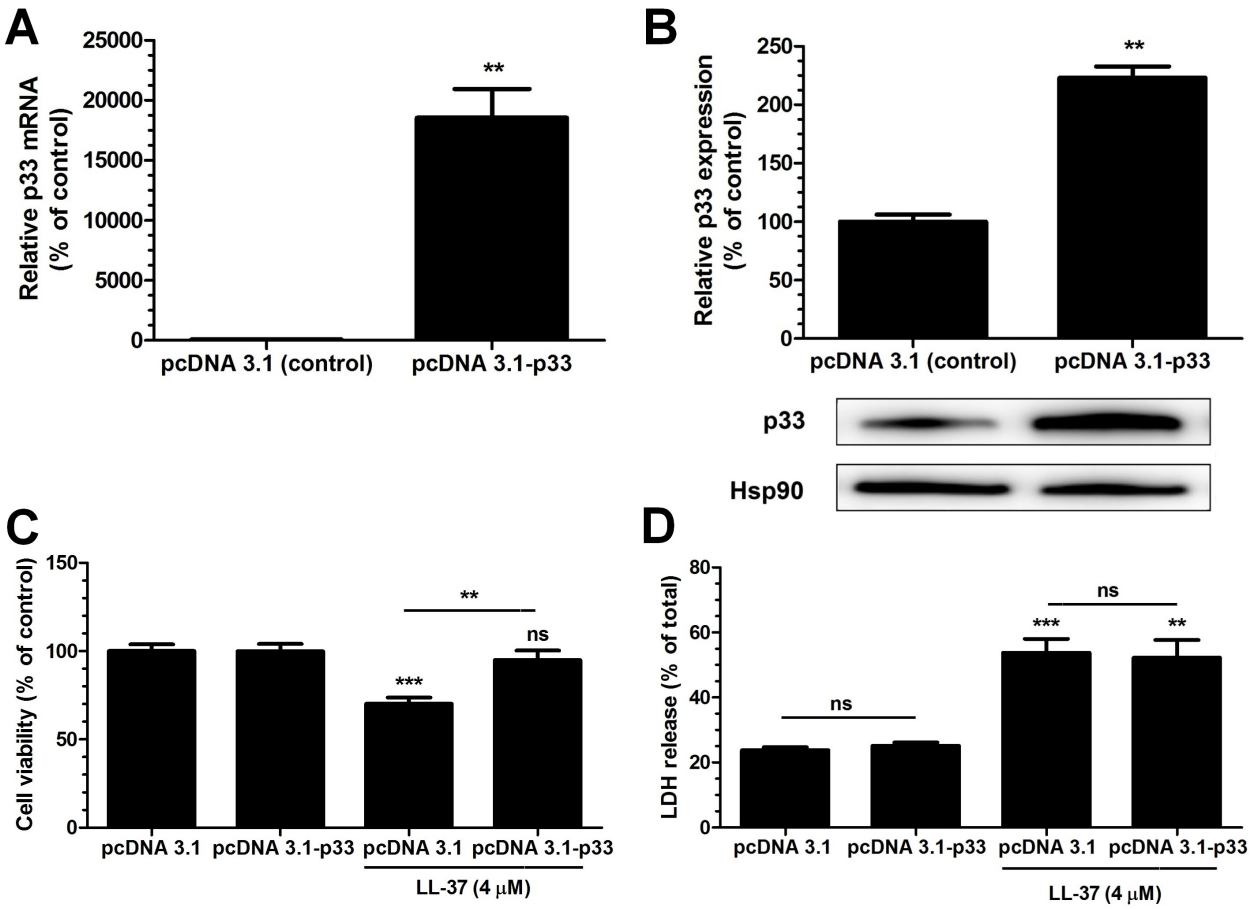
A
Relative p33 mRNA (% of control)
25000
20000
15000
10000
5000
0
**
pcDNA 3.1 (control)
pcDNA 3.1-p33
B
Relative p33 expression (% of control)
250
200
150
100
50
0
**
pcDNA 3.1 (control)
pcDNA 3.1-p33
p33
Hsp90
C
Cell viability (% of control)
150
100
50
0
**
ns
***
pcDNA 3.1
pcDNA 3.1-p33
pcDNA 3.1
pcDNA 3.1-p33
LL-37 (4 μM)
D
LDH release (% of total)
80
60
40
20
0
ns
***
**
ns
pcDNA 3.1
pcDNA 3.1-p33
pcDNA 3.1
pcDNA 3.1-p33
LL-37 (4 μM)

Figure 9

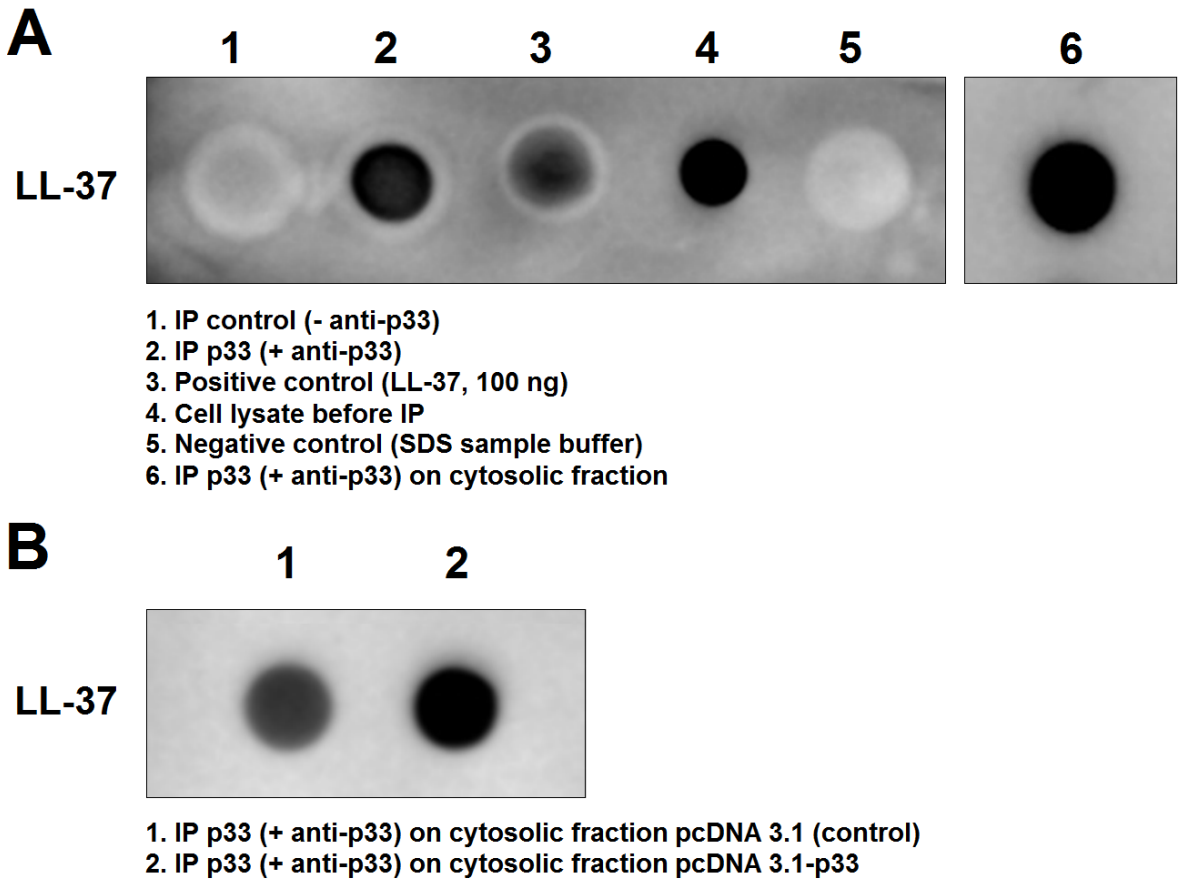
A
1
2
3
4
5
6
LL-37
1. IP control (- anti-p33)
2. IP p33 (+ anti-p33)
3. Positive control (LL-37, 100 ng)
4. Cell lysate before IP
5. Negative control (SDS sample buffer)
6. IP p33 (+ anti-p33) on cytosolic fraction
B
1
2
LL-37
1. IP p33 (+ anti-p33) on cytosolic fraction pcDNA 3.1 (control)
2. IP p33 (+ anti-p33) on cytosolic fraction pcDNA 3.1-p33

Figure 10

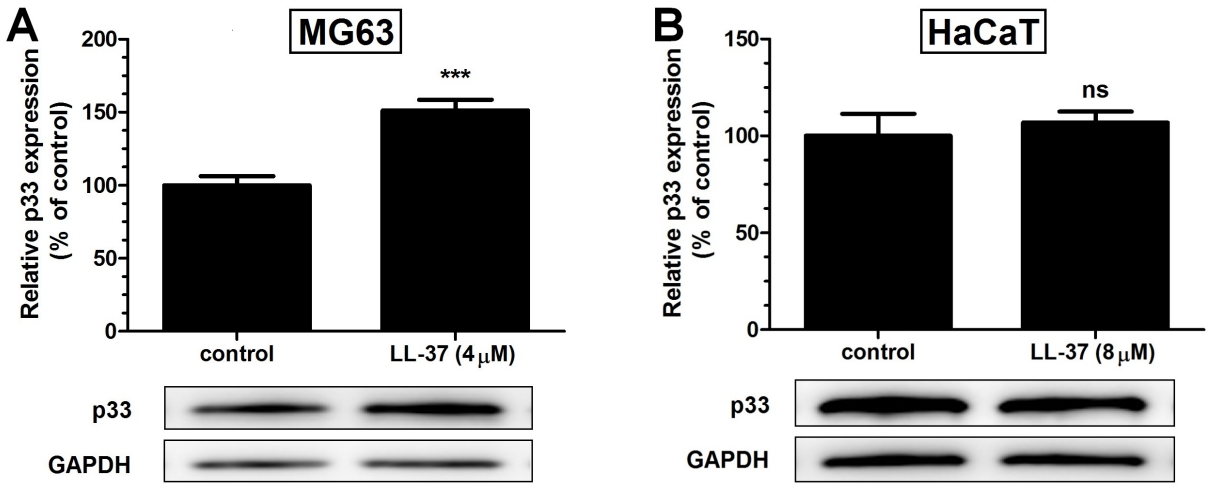
A
MG63
Relative p33 expression (% of control)
200
150
100
50
0
***
control
LL-37 (4 μM)
p33
GAPDH
B
HaCaT
Relative p33 expression (% of control)
150
100
50
0
ns
control
LL-37 (8 μM)
p33
GAPDH